 doi:10.20944/preprints201911.0395.v1

Article

Cardiac Hypertrophy in a Dish: A Human Stem Cell Based Model

Markus Johansson [1,2]*, Benjamin Ulfenborg[1], Christian X Andersson[3], Sepideh Hagvall[1,4], Anders Jeppsson[2,6], Peter Sartipy [1,5] and Jane Synnergren [1]

[1] Systems Biology Research Center, University of Skövde, SE-541 28 Skövde, Sweden
[2] Department of Molecular and Clinical Medicine, Institute of Medicine, The Sahlgrenska Academy at University of Gothenburg, Gothenburg, Sweden
[3] Takara Bio Europe AB, Gothenburg, Sweden
[4] Bioscience, Research and Early Development, Cardiovascular, Renal and Metabolism (CVRM), BioPharmaceuticals, R&D AstraZeneca, Gothenburg, Sweden
[5] Late-stage Development, Cardiovascular, Renal and Metabolism (CVRM), BioPharmaceuticals R&D, AstraZeneca, Gothenburg, Sweden
[6] Department of Cardiothoracic Surgery, Sahlgrenska University Hospital, Gothenburg, Sweden.

* Correspondence: markus.johansson@his.se

Abstract:

Cardiac hypertrophy is an important and independent risk factor for the development of heart failure. To better understand the mechanisms and regulatory pathways involved in cardiac hypertrophy, there is a need for improved in vitro models. In this study, we investigated how hypertrophic stimulation affected human induced pluripotent stem cell (iPSC)-derived cardiomyocytes (CMs). The cells were stimulated with endothelin-1 (ET-1) for 8, 24, 48, 72, or 96h. Parameters including cell size, ANP-, proBNP-, and lactate concentration were analyzed. Moreover, transcriptional profiling using RNA-sequencing was performed to identify differentially expressed genes following ET-1 stimulation. The results show that the CMs increase in size by approximately 13% when exposed to ET-1 in parallel to increases in ANP and proBNP protein and mRNA levels. Furthermore, the lactate concentration in the media was significantly increased indicating that the CMs consume more glucose, a hallmark of cardiac hypertrophy. Using RNA-seq, a hypertrophic gene expression pattern was also observed in the stimulated CMs. Taken together, these results show that hiPSC-derived CMs stimulated with ET-1 display a hypertrophic response. The results from this study also provide new molecular insights about the underlying mechanisms of cardiac hypertrophy and may help accelerate the development of new drugs against this condition.

Keywords: cardiac hypertrophy; cardiomyocytes; disease model; endothelin-1; stem cells

1. Introduction

Cardiac hypertrophy is characterized by an enlargement of the heart due to an increase in size of the cardiomyocytes (CMs) (*1*). There are two major types of cardiac hypertrophy; physiological and pathological. Physiological hypertrophy is naturally occurring during post-natal growth, pregnancy and exercise (*2-4*). It is reversible and does not progress to clinically overt heart failure. Pathological hypertrophy, on the other hand, may progress to heart failure if the stimuli persists for an extended time and is a maladaptive decompensatory condition where the heart increases in size due to alteration in several signaling pathways (*5-7*). These alterations result in pathological

 doi:10.20944/preprints201911.0395.v1

hypertrophy including adverse gene expression profile, increase in ANP and BNP protein levels, and increased lactate production due to a higher glucose consumption (*8-10*). This type of cardiac hypertrophy is induced by conditions such as chronic hypertension, aortic stenosis, myocardial infarction, or gene mutations. Until recently, only animal-based models have been available to study cardiac hypertrophy in a pre-clinical setting. These models are in many ways useful, but there are significant differences between human- and animal- cardiovascular systems, including stress response and ion channel expression, that makes translation to the human situation challenging (*11*). Novel technologies, based on human stem cells, could offer clinically relevant in vitro-based alternatives.

Human pluripotent stem cells (hPSCs) have a unique capability to self-renew and differentiate into all cell types in the body (*12*). These features make them useful for various in vitro applications, such as toxicity testing and disease modeling. In particular, hPSC-derived CMs have proven to be useful in many in vitro assays (*13-15*). Human cell-based models are anticipated to provide alternatives to the use of animal models for studies of cardiac hypertrophy mechanisms. Besides providing systems that are scalable and may improve the translation of the results to the clinical situation, the availability of human cell-based models can also help to reduce the need for animal experiments.

Cardiac hypertrophy can be induced by different methods in vitro, where the most commonly used are neurohormonal stimulation and physical stretching. The neurohormonal approach uses substances that bind to specific receptors and activate signaling pathways that initiate changes in a series of compensatory mechanisms, involving heart rate, heart contractility, and salt and water retention (*16, 17*). All for trying to maintain the cardiovascular homeostasis. Commonly used substances for cardiac hypertrophy induction are ET-1 and phenylephrine (*18-20*). Both of these are vasoconstrictors; ET-1 being the most potent one (*21*). The stretch model uses mechanical force to induce hypertrophy. Several extracellular matrix sensing receptors, e.g. integrins and cytoskeletal filaments activate signaling pathways, which trigger a hypertrophic response (*22*). Both approaches have been shown to render a hypertrophic state in hPSC-derived CMs. The degree of response varies between studies, making definitive conclusions challenging. The different experimental settings used, including starting material, and the induction method, may help to explain these differences and there is a need for standardization between laboratories (*18-20, 22*). Currently, the reports on neurohormonal in vitro models for cardiac hypertrophy used today thus far lack information on how the hypertrophy is regulated over time. The stem cell-based models described to date typically use single time point stimulations and responses are usually analyzed within 24 hours (*18, 20*). Such models are suitable for assessing the acute responses but they do not provide information on how the hypertrophy response develops over time. Another critical component of the model is the cell source, as the CMs need to be of high quality and purity while possessing key cardiac functionalities. Extended culturing time has been shown to improve the maturation of the hiPSC-CMs and is therefore an important parameter to consider when developing an in vitro model based on such cells (*23*).

In this study, we have investigated the hypertrophic response over time in hiPSC-derived CMs. The CMs were stimulated with ET-1 during various time points and assessed the acute and long-term hypertrophic response were subsequently analyzed

2. Results

Preprints (www.preprints.org) | NOT PEER-REVIEWED | Posted: 30 November 2019 doi:10.20944/preprints201911.0395.v1

2.1. Cardiomyocyte homogeneity

The CMs used in this study were of high purity and showed a high proportion of cardiac troponin T (cTnT) positive cells throughout the experiments. The homogeneity of the CM cultures was analyzed with flow cytometry (FC) before cryopreservation at day 19 and 32 following start of differentiation. The results show that, prior to cryo-preservation at day 19, 97% of the cells were cTnT positive (data not shown) and the population of cells at day 32 contained 92% cTnT positive cells (Fig.1).

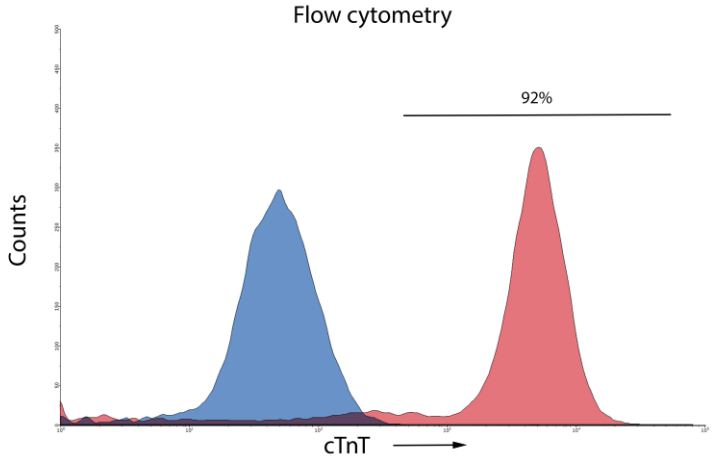

Figure 1. FC results. Histogram plot of the FC analysis performed on the CMs used in the study. The x-axis shows the number of counts and the y-axis shows the fluorescence intensity. Blue peak represents control and red peak represents the sample. The bar signifies the interval of cTnT+ cells.

In order to monitor the cells after thawing and ET-1 stimulation, we also performed immunocytochemistry (ICC) and stained the cells for cTnT (Red) and F-actin (Green) (Fig 2). Images were captured at 8, 24, 48, 72, and 96h after ET-1 stimulation. Images of control cells (incubated without ET-1) were also captured. The ICC analysis verified the FC results and demonstrates a high proportion of CMs in the cultures. The CM population remained stable over time and no difference in expression of cTnT could be observed over the course of the experiments.

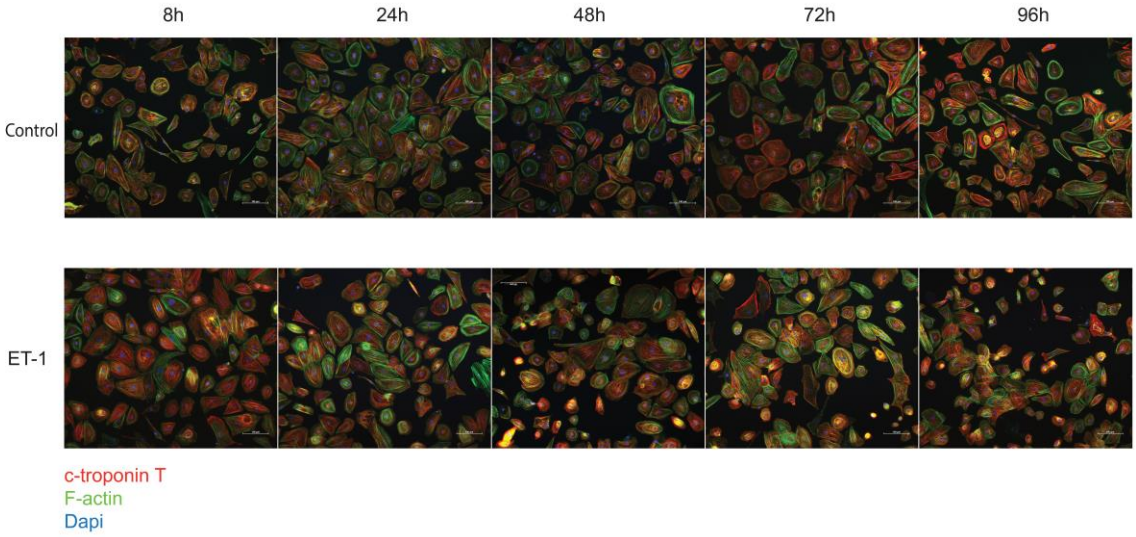

Figure 2. ICC images. Cardiomyocytes stained for c-troponin T (red), F-actin (green) and Dapi (blue). The first row of images shows control CMs and the second row ET-1 stimulated CMs, both groups at 8, 24, 48, 72 and 96h. Images were captured at 10x and the scale bar represents 100µm.

2.2. Gene expression

Preprints (www.preprints.org) | NOT PEER-REVIEWED | Posted: 30 November 2019 doi:10.20944/preprints201911.0395.v1

The response to ET-1 were both dependent on concentration and affected by the time in culture of the CMs. To determine the optimal concentration of ET-1, dose-response experiments were conducted and the gene expression levels of three commonly used hypertrophy markers (*NPPA*, *NBBP* and *ACTA1*) were analyzed (Fig 3). The experiments were performed on CMs cultured for 25 and 38 days after initiation of differentiation, in order to investigate if the time in culture had any effect on the hypertrophic response. The concentrations 0.1, 1.0, 10 and 100nM of ET-1 were used.

After ET-1 stimulation for 24h, *NPPA*, *NPPB* and *ACTA1* levels were all up-regulated in a dose-dependent manner. Maximal response was observed at 10nM ET-1. Notably, the response was more pronounced in CMs cultured for 38 days compared to cells at day 25 (Fig 3a-c). The gene expressions of *NPPB* and *ACTA1* were 9-fold and 12-fold increased respectively at 10nM at day 38 compared to day 25 ($p < 0.05$) (Fig 3b-c). The expression of *NPPA* was 2-fold higher at 10nM at day 38 compared to day 25, however not statistically significant (Fig 3a). Taken together, these data demonstrate that CMs cultured for 38 days produce a more robust hypertrophic response, as measured by gene expressions of key markers, compared to CMs at day 25. Based on these results, day 38 CMs and 10nM of ET-1 was used subsequently in all experiments in the following study.

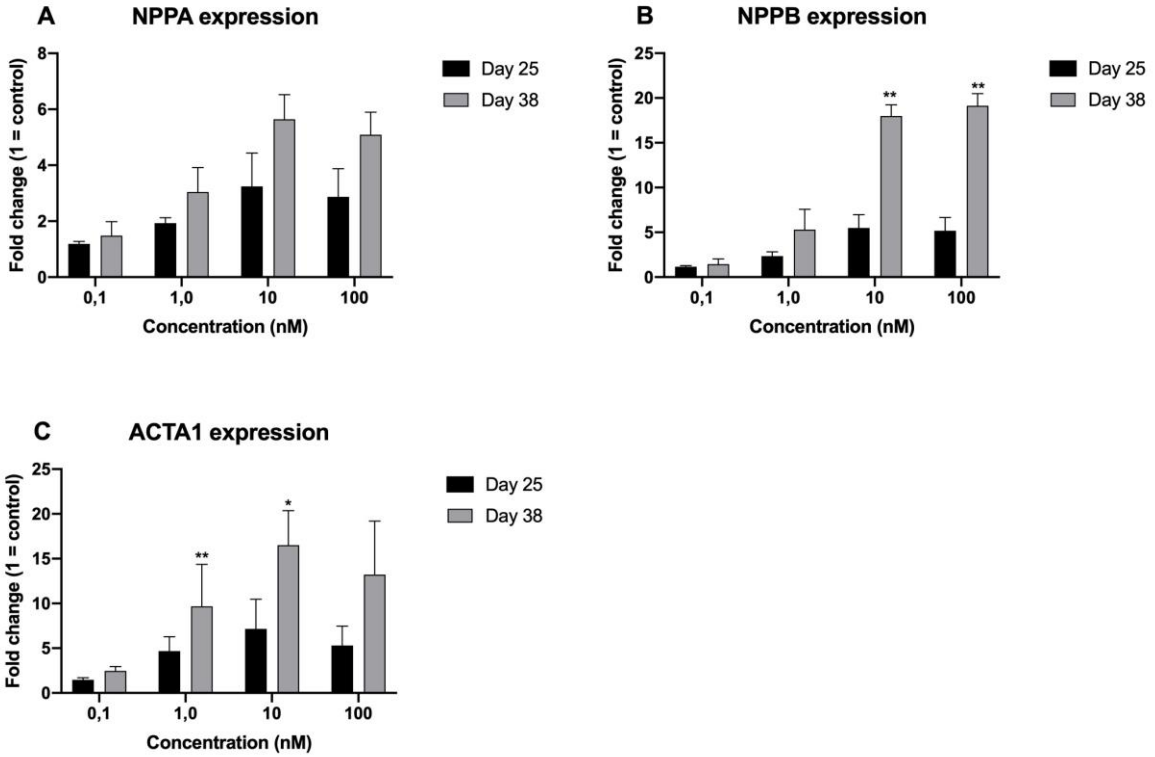

Figure 3. RT-qPCR results. Dose response experiment using CMs cultured to day 25 and day 38. The results are presented as relative fold change, normalized against the endogenous control CREBBP and unstimulated control CMs. A) NPPA expression B) NPPB expression C) ACTA1 expression. Standard deviation (SD) are given as error bars (n=3). * = $p<0.05$, ** = $p<0.01$.

2.3 Protein analysis

ET-1 stimulated CMs show an increased secretion of the natriuretic proteins ANP and proBNP. Incubation with ET-1 significantly upregulated the expression of ANP between 24 and 96h. After 8h of stimulation, there was no difference in ANP between control and ET-1 stimulated CMs. The increase was evident from 24h and onward. The highest concentration of ANP was observed after 48h and the concentration was more than 2-fold compared to the controls. After 48h and onwards, the ANP-concentration decreased slightly with each time point. However, still at 96h, the concentration of ANP was significantly higher compared to control. The control CMs showed a stable level of ANP protein during the entire experiments (Fig 4a).

Preprints (www.preprints.org) | NOT PEER-REVIEWED | Posted: 30 November 2019 doi:10.20944/preprints201911.0395.v1

Furthermore, proBNP was significantly upregulated at all the time points studied (8-96h), except for the 72h time point which did not reach statistical significance (p=0.056). Already after 8h the concentration of proBNP was more than 6-fold higher compared to controls. The maximum concentration was observed at 24h, representing a 9-fold increase compared to control. Repeated stimulation after 24h did not further increase the proBNP concentration. Instead, a decay at every time point after 24h was observed. Although decreased, the concentration was still significantly higher compared to control at the last time point studied (96h) (Fig 4b). The control CMs showed a stable level of proBNP protein during the entire experiments (Fig 4a-b).

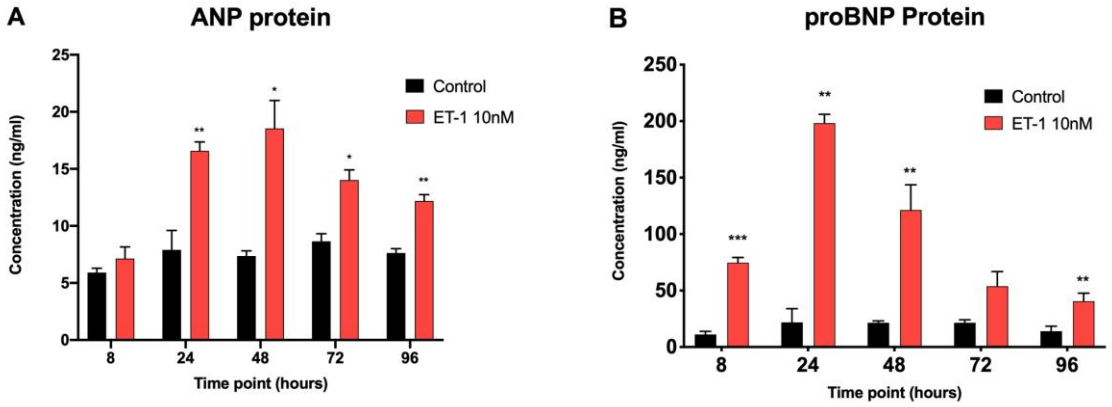

Figure 4. ANP and proBNP analysis in conditioned media. Red bars represent CMs stimulated with ET-1 and black bars represent control CMs. The x-axis shows the concentration in ng/ml and the y-axis the time points. A) Concentration of secreted ANP protein. B) Concentration of secreted proBNP protein. SD is given as error bars (n=3). * = p<0.05, ** = p< 0.01 *** p<0.001.

2.4 Lactate analysis

The lactate concentration in the culture media was significantly increased in the ET-1 stimulated CMs. Lactate concentration is an indirect measurement of the glucose consumption. Increased glucose consumption is an important feature of the hypertrophy response. The lactate concentration in the ET-1 stimulated CMs was over 2.5-fold compared to control cells at the 24, 48, 72 and 96h time points (Fig 5). The mean lactate concentration in the media at those time points were 586ng/ul (479 – 727ng/ul) compared to 240ng/ul (188-247ng/ul) in the controls (p<0.0001). An increase was observed already at the 8h time point, albeit not statistically significant. The rate of which lactate was produced was similar at all time points, indicating that the increase in glucose consumption is an immediate effect of stimulation with ET-1.

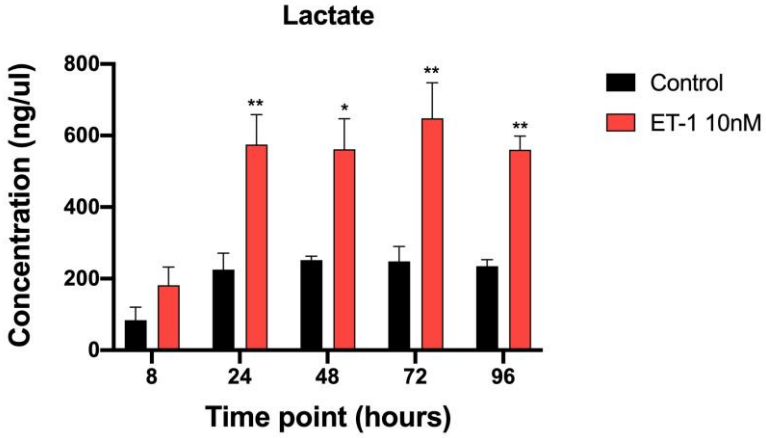

Figure 5. Lactate concentration analysis in conditioned media. The x-axis shows the concentration of lactate in ng/ul and the y-axis the time points. Red bars represent CMs stimulated with ET-1 and black bars represent control CMs. SD is given as error bars (n=3). * = p<0.05, ** = p< 0.01.

Preprints (www.preprints.org) | NOT PEER-REVIEWED | Posted: 30 November 2019 doi:10.20944/preprints201911.0395.v1

2.5 Cell size

The increase in CM cell size was evident after 24h of stimulation with ET-1. Cell size was analyzed in living cells at several time points. At 8h of stimulation with ET-1, there was no significant change in cell size compared to controls. However, at 24h, the ET-1 stimulated CMs displayed an increased volume compared to 8h of stimulation (5.64μm^3 (4.75 – 5.04 μm^3) vs 4.92μm^3 (5.35 – 5.86μm^3), $p<0.01$) and was significantly larger than the control CMs which had a volume of 5.05μm^3 (4.51 – 5.35μm^3), $p=0.04$. At 48, 72 and 96h of stimulation, the ET-1 stimulated CMs had a significantly increased volume by an average of 0.87μm^3 (13%) compared to controls ($p<0.0001$) (Fig 6). No further increase in size was detectable after 48h. The control CMs remained at approximately the same size at every time point throughout the experiments.

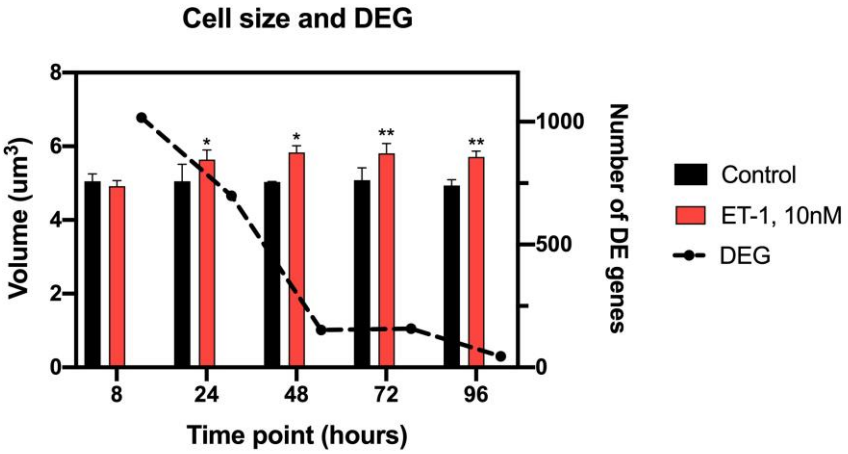

Figure 6. Cell size. The graph shows the cell size and the number of DEG. The bars represent the cell volume. Black bars are controls and red bars represent stimulated cells. The dotted line shows the number of DEG. The left y-axis shows the volume, the right y-axis the number of DEG, and the x-axis the different time points.

2.6 Transcriptional profiling

Transcriptional profiling of ET-1 stimulated CMs revealed a robust hypertrophic response. Gene expression profiles obtained by RNA-seq analysis at 8, 24, 48, 72, and 96h of ET-1 stimulation were investigated. This analysis identified 1017, 699, 152, 158, and 45 differentially expressed (2-fold, $p<0.05$) genes at 8, 24, 48, 72, and 96h respectively (Fig 7). Interestingly, the cell size did not correlate with the number of differentially expressed genes (DEG). The cell size was maintained from 24 to 96h while the number of DEG decreased over this time period (Fig 6).

Hierarchical clustering shows a clear separation of all the ET-1 treated samples and the control samples. At the 8, 24, and 48h time points, the numbers of upregulated and downregulated genes were in similar range (Fig 7a-c). However, at the later time points (72h and 96h) the majority of DEG were upregulated by the ET-1 stimulation (Fig 7d-e).

Preprints (www.preprints.org) | NOT PEER-REVIEWED | Posted: 30 November 2019 doi:10.20944/preprints201911.0395.v1

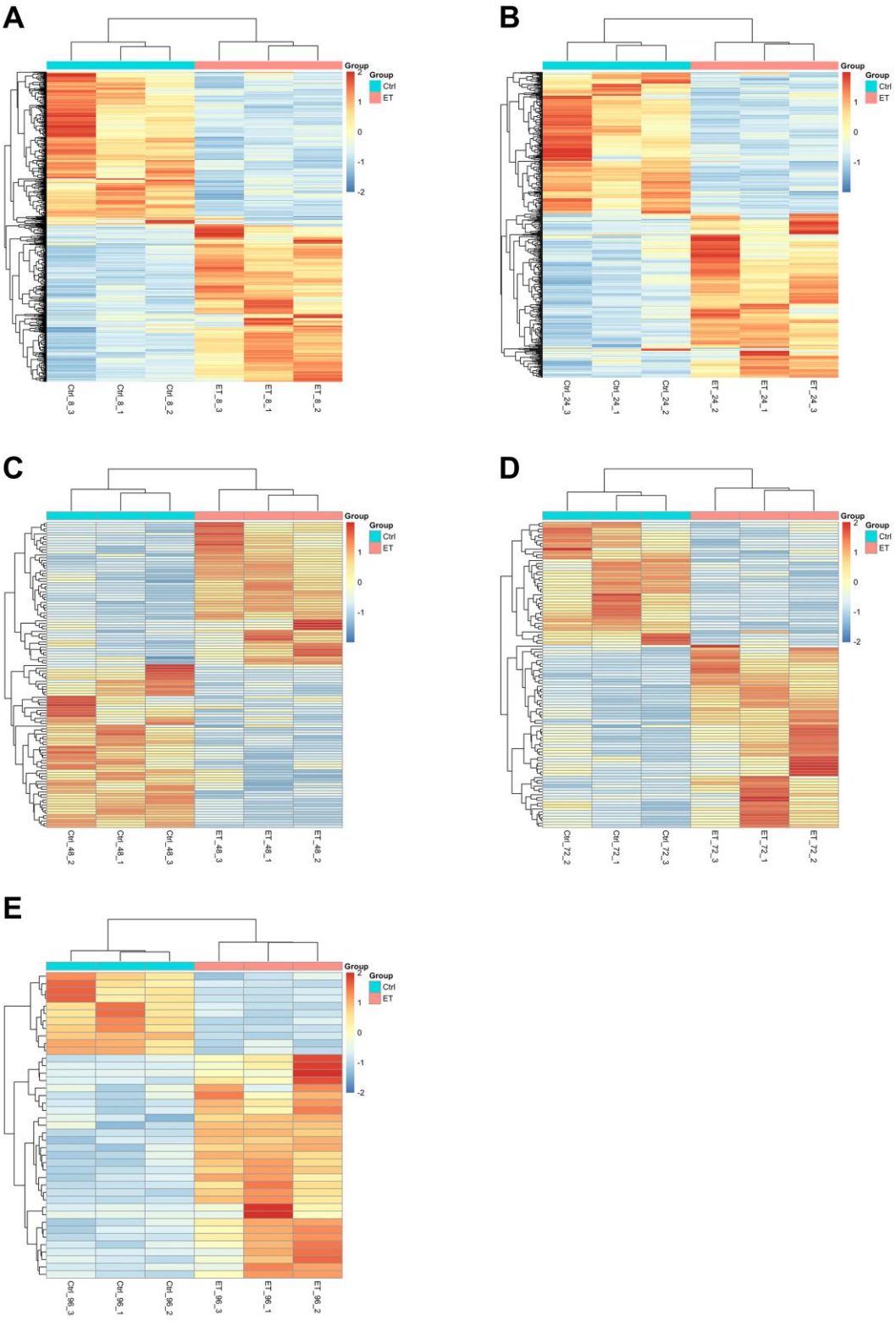

Figure 7. Heatmaps and hierarchical clustering of all DEG (rows as genes and columns as samples). The color indicates gene expression with highest expression values in red and lowest expression values in blue. A) 8h B) 24h C) 48h D) 72h E) 96h.

Preprints (www.preprints.org) | NOT PEER-REVIEWED | Posted: 30 November 2019 doi:10.20944/preprints201911.0395.v1

The Venn diagrams (Fig 8a-b) describe the overlap of significantly upregulated and downregulated genes at the different time points. For the upregulated genes, only 5 genes were overlapping between all the time points. The largest overlap (121 genes) was observed between the 8h and 24h time points (Fig 8a). The same trend was evident for the downregulated genes with only 2 overlapping genes across all the time points. The highest number of overlapping DEG that show downregulation (141 genes) was observed between time point 8h and 24h (Fig 8b).

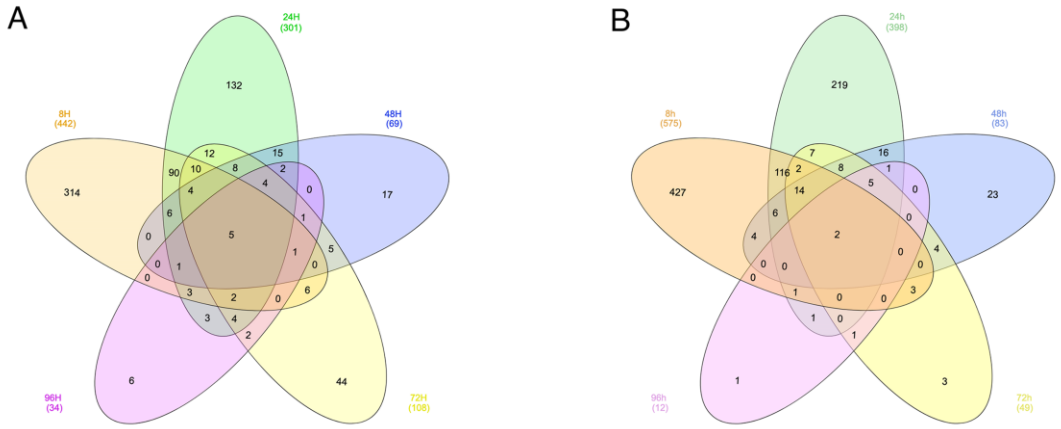

Figure 8. Venn diagram that shows the number of unique and overlapping genes, either upregulated (A) or downregulated (B) by ET-1 stimulation.

A GO enrichment analysis was performed applying the Cytoscape software and the ClueGO plugin on the list of upregulated genes in each time point respectively. In addition to enrichment of specific terms related to cardiac hypertrophy, such as muscle structure development, the GO enrichment results show a broad response of various functions from the ET-1 stimulation at the early time points, 8 to 24h (Supp. Fig 1a-b). At the 24h time point, there was still a relatively broad response shown among the enriched GO terms but also many GO terms specifically related to cardiac hypertrophy (muscle contraction, extracellular structure organization, myofibril assembly and structural constituent of cytoskeleton) were enriched (Supp. Fig 1b). At the later time points 48, 72 and 96h, fewer enriched GO terms were observed, but on the other hand these were highly relevant in terms of the cardiac hypertrophy mechanism (Supp. Fig 1c-e). These results are in line with the data showing a broad response in the cells at the beginning of the ET-1 stimulation and a more specific effect is observed after 48h of stimulation. This indicates that the CMs to some extent adapt to stimulation of ET-1.

To further explore the transcriptional profiles of genes of specific relevance for muscle tissue, 398 genes annotated with the GO term 'muscle system processes' (GO level 4) where selected and explored in more detail. The number of genes assigned with this term and that show differential expression in our data was calculated. In total 24, 24, 10, 9, and 6 genes at the time points 8, 24, 48, 72 and 96h respectively (Fig 9a-e) were annotated with this GO term and were differentially expressed in the ET-1 stimulated cells. We also explored genes more specifically annotated with 'cardiac muscle hypertrophy in response to stress' which are of very high relevance for this disease model such as *NPPA*, *NPPB* and *BMP10* and these are all differentially expressed in the ET-1 stimulated cells. *NPPA* is differentially expressed at all investigated time points and *NPPB* at 8, 24 and 72h (Fig 9a-c). *BMP10* is only differentially expressed at the 8h time point (Fig 9a). Cardiac hypertrophy is associated with alterations in calcium handling and hence, it is reassuring that genes encoding for proteins involved in calcium handling and signaling (*CACNA1D*, *CACNA1G*, *CACNA1S* or *CASC2*) also show differential expression at all time points in our model (Fig 9a-e).

Preprints (www.preprints.org) | NOT PEER-REVIEWED | Posted: 30 November 2019 doi:10.20944/preprints201911.0395.v1

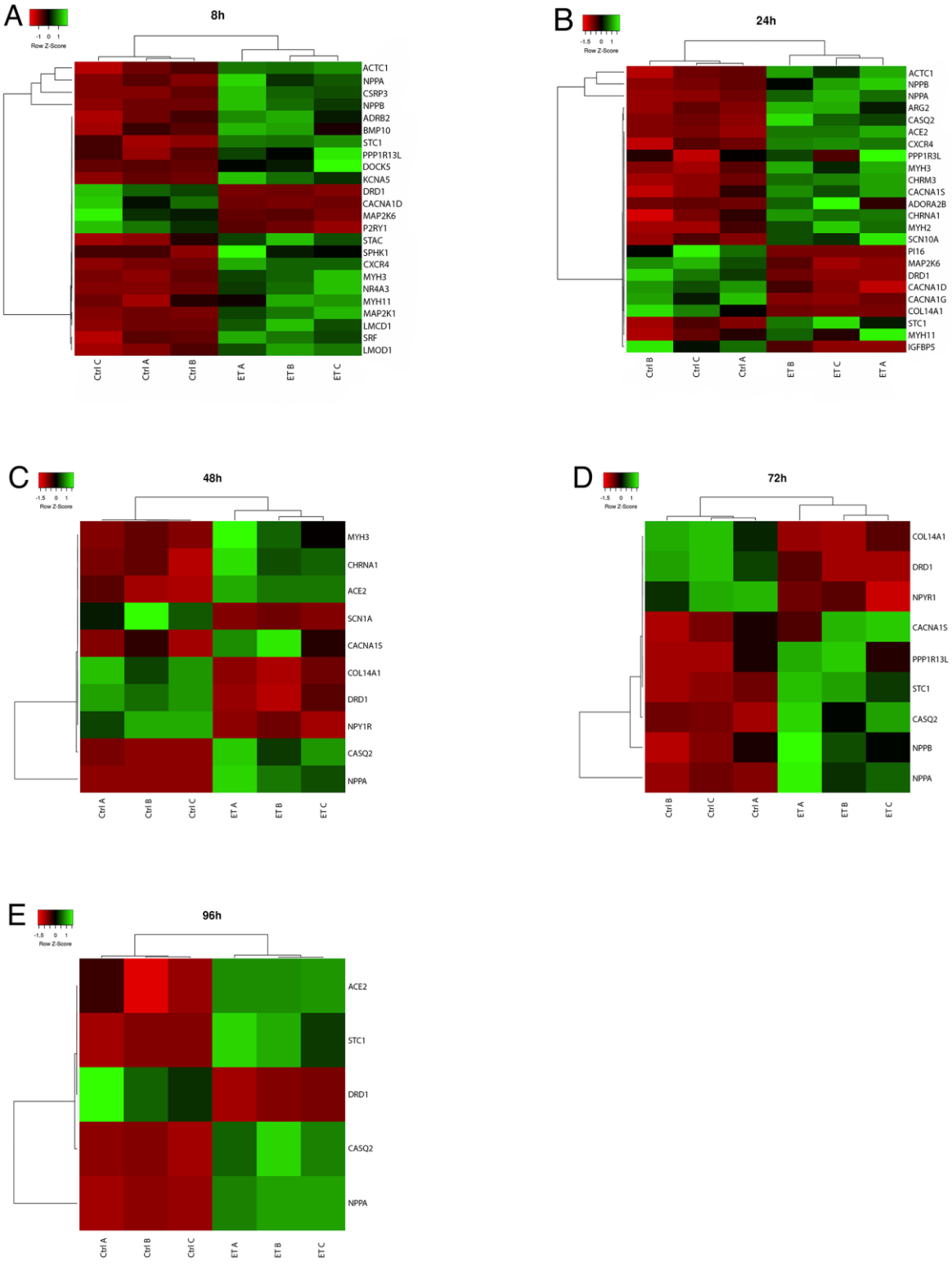

Figure 9. Heatmaps of DEG annotated with the GO term GO:0003012 (muscle system process) at the different time points and that are differentially expressed. The scale goes from red to green with the lowest z-score as red and the highest as green. The rows represent the DEG found in the GO term and the columns represent the samples. A) 8h B) 24h C) 48h D) 72h E) 96h.

 doi:10.20944/preprints201911.0395.v1

3. Discussion

In this study, we have exposed hiPSC-derived CMs to ET-1, a known hypertrophic substance, and evaluated the response with various methods. The model shows a robust response to ET-1. We identified upregulation at both gene and protein levels, of the natriuretic proteins ANP and proBNP in the stimulated CMs. Physical parameters such as cell size increased during the first 24h and stayed increased throughout the experiments. The same observation was evident regarding lactate production in the cells. We also used RNA-seq to assess the global gene expression changes in the cells following ET-1 stimulation. Interestingly, a substantial and broad response was observed at the early time points of stimulation. However, the CMs seem to adapt to the ET-1 stimulation over time and the initial broad response transforms into a more focused response characteristic of cardiac hypertrophy.

The starting cell material is of great importance in all cell biology studies and it is known that extended culture of CMs can enhance their functionality (*23*). Therefore, we chose to assess the utility of CMs that had been differentiated and cultured for various time periods (i.e., 25 and 38 days). We performed real-time qPCR analysis and measured the expression of a few key hypertrophy genes (*NPPA, NPPB* and *ACTA1*) to elucidate if time in culture affects the hypertrophic response. The results clearly showed a difference in response between the day 25 and day 38 CMs. This is in line with results from other studies where extended culture of the CMs also showed enhanced maturation of the cells (*23-25*). The difference in response related to time in culture can probably be one explanation of why there is a discrepancy among the data reported previously regarding hypertrophic responses in stem cell-derived CMs (*26, 27*).

In this work we tested four different concentrations of ET-1 (0.1, 1.0, 10 and 100nM) to determine the optimal concentration for hypertrophy induction. The results show that 10nM gave optimal response in terms of gene expression of *NPPA*, *NPPB* and *ACTA1*. These results are in line with data from other studies that have used ET-1 to induce hypertrophy (*19, 20, 28*). We also tested different durations of ET-1 stimulation between 8h and 96h. To our knowledge, this has not previously been reported with hiPSC-derived CMs using the neurohormonal induction method. Using the stretch-induced method, differences have been shown in the response depending on duration of mechanical force. Forty-eight hours seems to be the most suitable duration of stimulation when conducting those types of hypertrophy experiments (*18, 29*). Human iPSC-based models using ET-1 have no comprehensive data available from the very early time of stimulation and most of the studies are conducted between 18 to 48h of stimulation. Rat models have on the other hand been tested with longer ET-1 stimulation and results from these studies show that the time of stimulation have a great impact on the hypertrophy response (*28*). In line with this, our results also demonstrate that the time of stimulation have a significant effect of the hypertrophy response also in human cells. Initially, the response is broad and the highest number of differentially expressed genes are identified at the first time point we tested (i.e., 8h) (Fig 6). This observation is of importance since it can give more insight into the initiation phase of the hypertrophy response. At this early time point, we could not observe any increase in cell size. The increase in size was initially observed after 24h, which is also in agreement with results from other studies (*18, 19*). However, those studies only present data from 24-48h of stimulation. Possibly, 8h is not long enough for the CMs to produce and organize the new proteins that are necessary for a cell size increase and that may be the reason why we only observe the effect on a transcriptional level at this time point. Based on this, we can conclude that the time of stimulation is an important factor to consider when developing a hypertrophy disease model. A shorter stimulation is more suitable for investigations of the initial response before any detectable changes in cell size have occurred. Stimulation time points at, or beyond, 24h appear more appropriate if the aim is to correlate molecular pathways with changes in cell size.

Thus far, there are no reports on how gene expression is regulated over time when hiPSC-derived CMs are stimulated repeatedly from 8h to 96h with ET-1. There is also a lack of data in the literature from the early phase (8h) of hypertrophy induction. Interestingly, we found that the highest number of DEG was observed at the 8h time point. We could also show that, at this time point, most DEG associated with the GO term muscle system processes. These novel findings reveal that, on a

 doi:10.20944/preprints201911.0395.v1

gene level, the hypertrophic response is apparent early, which can hopefully result in a better mechanistic understanding of the initiation of hypertrophy. Possibly, this may also represent a state where therapeutic interventions may have their best opportunity to slow down or stop the progression of pathological cardiac hypertrophy. Using this model for target identification may provide novel avenues for drug discovery.

To focus our analysis, 399 genes annotated with the broader term 'muscle system process' including genes involved in muscle adaption, muscle contraction, muscle hypertrophy, regulation of muscle system process and relaxation of muscle were selected and analyzed in more detail. Ten percent of all genes annotated with this GO term was identified as DEG in the ET-1 stimulated samples.

The gene expression data obtained from the RNA-seq analysis included many DEG that are important for the development of heart diseases. *ANKDR1* is 2.1-fold upregulated in our dataset. It is a transcription factor that is important in the myofibrillar stretch-sensor system. This marker has been found to be increased in patients with cardiomyopathy (*30*). Upregulation of this gene has been shown in stretch-induced in vitro models and our model replicates this finding (*22, 31*). Another important gene that is observed to be upregulated in patients with heart failure is *FSTL3* (*32*). This gene is involved in cardiac remodeling, which is a hallmark of cardiac hypertrophy. Knock down of this gene results in reduced cardiac hypertrophy in rats when exposed to hypertrophic agents (*33*). In our model, the *FSTL3* gene is significantly upregulated, showing that the model can mimic the in vivo counterpart. One of the highly upregulated genes in our data set was *IL-11*. It has been shown to be important for the development of fibrosis and is increased in patients with heart failure (*34, 35*). Inhibiting interleukin 11 could possibly be an effective treatment against several forms of heart diseases and our model could potentially be used for such investigations (*36*).

In this study, we have developed an in vitro model that can be used to study cardiac hypertrophy and potentially serve as a suitable platform for drug screening. We used one human cell line to generate the CMs. For future studies it would be of interest to assess several cell lines, including cell lines derived from donors with genetic disorders associated with cardiac hypertrophy, to investigate possible differences in the hypertrophic response that may be cell line dependent. It would also be of interest to benchmark the model against human primary CMs stimulated with ET-1. However, the availability of primary human CMs is very limited, and they are difficult to maintain in culture. There is an urgent need for novel drugs targeting cardiovascular diseases, and stem cell-based models may provide new alternatives for drug discovery. Our model described here shows a robust hypertrophic response following incubation with ET-1, and it could possibly be used to screen for new drug candidates. It appears also to be suitable for dissecting the signals responsible for initiation and progression of cardiac hypertrophy in order to improve our understanding of the molecular mechanisms underlying the development of cardiac hypertrophy.

4. Materials and Methods

4.1 Cardiomyocytes

Human CMs derived from the hiPSC line ChiPSC22 were obtained from Takara Bio (Takara Bio Europe AB). The CMs were cryopreserved at day 19 and day 32 following onset of differentiation using the STEM-CELLBANKER® (cat 11890, Amsbio).

4.2 Flow cytometry

In conjunction with the cryopreservation, 1 million cells were collected and used for flow cytometry analysis. In short, cells were fixed in paraformaldehyde (HistoLab products AB), resuspended in methanol (-20°C) (cat 311415, Sigma Aldrich) and stained for cardiac troponin T using Anti-cardiac Troponin T antibody (ab45932, Abcam) as primary antibody and Alexa flour 488 Fab2 goat anti rabbit IgG antibody (ab150077, Invitrogen,) as secondary antibody. The analysis was performed using a Guava® easyCyte HT Sampling Flow Cytometer (Merck Millipore).

 doi:10.20944/preprints201911.0395.v1

4.3 Hypertrophy induction

Cryopreserved CMs (from day 19 and 32 of differentiation) were thawed in CM medium (Advanced RPMI, B27 1x, Glutamax 1x, (ThermoFisher)) supplemented with Y27632 (10μM) (cat Y0503, Sigma-Aldrich) and plated at 3.0 x 10^5 cells/well in 48-well plate precoated with 5μg/cm^2 Fibronectin solution (5μg/cm^2) (cat F0895, Sigma-Aldrich).

One day after thawing, the culture medium was changed to CM medium and cells were recovered for a total of 6 days before starting the experiments with ET-1. Medium (0.4ml/cm^2) was changed every second day. Dose response experiments were initially conducted to determine the optimum concentration of ET-1. ET-1 powder (cat E7764, Sigma-Aldrich) was dissolved in DMSO and then added to the culture medium. The corresponding volume of DMSO was added to the control cells in parallel. For the dose-response experiment, cells were stimulated for 24h. Subsequently, time response experiments were conducted by stimulating the CMs during different time periods. CMs that were incubated with ET-1 for more than 24h received fresh medium with ET-1 every 24h. All experiments were performed in triplicates and repeated three times.

4.4 Real-time qPCR

The cells were lysed and stored in RNAprotect (cat 76526, QIAGEN) at -20°C until extraction. Total RNA was extracted using MagMAX™ Total RNA Isolation Kit (AM1830, Invitrogen, www.thermofisher.com) according to the manufacture's instructions and quantified by UV spectrophotometry on NanoDrop ND-1000 (NanoDrop). The quality of the RNA was verified using a 2100 Agilent Bioanalyzer. For RNA expression level analysis, RNA was converted to cDNA using High-Capacity cDNA Reverse Transcription Kit (4368814, Applied Biosystems). RT-qPCR was performed using Taqman Gene expression assays (*ACTA1* Hs00559403_m1, *NPPA* Hs00383230_g1, *NPPB* Hs00173590_m1) (ThermoFisher) on a 7500 Fast Real-time PCR system (Applied biosystems). Fold change values were calculated using the delta-delta CT method normalized to the CREBBP gene (Hs00173590_m1) (*37*).

4.5 Immunocytochemistry

The cells were fixed and stained according to a previously described protocol (*38*). Briefly, cells were fixed with paraformaldehyde (HistoLab products AB) and stained for cardiac troponin T (anti cardiac troponin T antibody, ab45932, abcam), F-actin (Phallodin (Alexa Flour 488 Phalloidin, A12379, ThermoFisher Scientific) and DNA (DAPI, cat 62248, ThermoFisher Scientific). Images were captured with a fluorescent microscope (Eclipse TE2000-U, Nikon).

4.6 ANP and proBNP ELISA and lactate assay

Conditioned cell culture media was collected at different time points. The media was centrifuged (5000xg, 5 minutes) and the supernatant collected and stored at -80°C for subsequent analysis. ANP and proBNP were measured using ELISA kits (EHPRONPPB and EIAANP, ThermoFisher Scientific) according the manufacture's instructions. Lactate measurements were performed with Lactate Assay kit II (cat MAK065, Sigma-Aldrich) according to the manufacture's instructions. Standard curve, cell size and concentration calculations were performed using GraphPad Prism 8 (GraphPad Software Inc).

4.7 Cell size

Cell volume measurements were performed on live cells using a Moxi Z mini automated cell counter (Orflo, www.orflo.com) with M cassettes. The medium was aspirated and the cells harvested using Trypsin/EDTA, centrifuged, resuspended in 0.5ml DPBS (Gibco, www.ThermoFisher.com) and analyzed using the Moxi Z instrument. Cells with a diameter between 12-34uM were included in the analysis.

 doi:10.20944/preprints201911.0395.v1

4.8 RNA-seq analysis

Library construction was performed using Illumina Truseq stranded total RNA with Illumina Ribozero method. Clustering was done by 'cBot' and samples were sequenced on NovaSeq6000 (NovaSeq Control Software 1.6.0/RTA v3.4.4) with a 2x51 setup using 'NovaSeqXp' workflow in 'S1' mode flowcell. The Bcl to FastQ conversion was performed using bcl2fastq_v2.19.1.403 from the CASAVA software suite. The quality scale used was Sanger / phred33 / Illumina 1.8+. Processing of FASTQ files was carried out by the SciLifeLab National Genomics Infrastructure at the Uppsala Multidisciplinary Center for Advanced Computational Science, Sweden. Sequenced reads were quality controlled with the FastQC software and pre-processed with Trim Galore. Processed reads were then aligned to the reference genome of Homo sapiens (build GRCh37) with the STAR aligner. Read counts for genes were generated using the featureCounts library and normalized FPKM values calculated with StringTie. Technical documentation on the RNA-seq pipeline can be accessed here: https://github.com/SciLifeLab/NGI-RNAseq. Raw and processed data are available for download at ArrayExpress (https://www.ebi.ac.uk/arrayexpress/) accession number: E-MTAB-8548.

4.9 Transcriptomics analysis

4.9.1 Differential expression analysis

The gene count data including 63,677 transcripts and 30 samples were imported into R (*39*) for further analysis, and statistical testing for differential expression was carried out with the quasi-likelihood F-test in the edgeR package (*40*). Only genes with a 2-fold change (FC) were included in the results. A false discovery rate (FDR) rate of ≤ 0.05 was considered statistically significant.

To explore the overlap of DEGs between the time points, Venn diagrams of upregulated and downregulated genes respectively, were generated using InteractivVenn (*41*). Heatmaps of selected sets of genes were generated using the R package pheatmap. DEG were identified among genes annotated with the GO term GO:0003012 and the more specific GO term GO:0014898. These DEG were used as input to Heatmapper to create heatmaps.

4.9.2 GO enrichment analysis

Gene Ontology (GO) enrichment analysis was performed using the Cytoscape software (version 3.7.1) and the ClueGO plugin (version 2.5.4). A two-sided hypergeometric test was applied with Bonferroni correction for multiple testing. GO terms at level 3-8 were included in the analysis and only terms with at least 4 genes with that annotation were considered. As reference set for the hypergeometric test all genes in selected ontologies were used.

4.10 Statistical analysis

Statistical analyses of RNA (real-time qPCR), protein, lactate and cell size measurements were justified using paired sample t-test. A p-value < 0.05 was considered statistically significant. The results are expressed as mean ±SD.

Supplementary Materials: Supplementary materials can be found online. **Figure S1.** Pie charts from ClueGO analysis. Input data are upregulated DEG. The pie charts show significantly overrepresented GO terms as % terms per group at the different time points. A) 8h B) 24h C) 48h D) 72h E) 96h.

Author Contributions: Conceptualization, C.X.A, P.S, S.H, A.J and J.S.; methodology, M.J, S.H, P.S, J.S.; validation, C.X.A, P.S, S.H and J.S.; formal analysis, M.J, BU; investigation, C.X.A, P.S, S.H, A.J and J.S.; resources, C.X.A and J.S; data curation, M.J; writing—original draft preparation, M.J, P.S, J.S.; writing—review and editing, M.J, C.X.A, S.H, P.S, J.S, A.J, BU; visualization, M.J, P.S, J.S.; supervision, A.J, P.S, J.S; funding acquisition, J.S.

Funding: This work was supported by the Systems Biology Research Centre at University of Skövde under grants from the Knowledge Foundation [2014/0301, 2016/0294 and 2016/0330], Takara Bio Europe, Gothenburg, Sweden, and AstraZeneca R&D, Gothenburg.

Conflicts of Interest: C.X.A. is an employee at Takara Bio Europe. P.S. and S.H. are employees at AstraZeneca. The other authors declare no conflict of interest.

Abbreviations

CM	Cardiomyocyte
CTnT	Cardiac troponin T
CVD	Cardiovascular disease
DEG	Differentially expressed genes
ET-1	Endothlin-1
FC	Flow cytometry
GO	Gene Ontology
ICC	Immunocytochemistry
IPSC	Induced pluripotent stem cell
RNA-seq	RNA sequencing
SD	Standard deviation

References

1. N. Frey, H. A. Katus, E. N. Olson, J. A. Hill, Hypertrophy of the Heart. *Circulation* **109**, 1580-1589 (2004).
2. B. M. Pluim, A. H. Zwinderman, A. van der Laarse, E. E. van der Wall, The athlete's heart. A meta-analysis of cardiac structure and function. *Circulation* **101**, 336-344 (2000).
3. M. Eghbali *et al.*, Molecular and functional signature of heart hypertrophy during pregnancy. *Circ Res* **96**, 1208-1216 (2005).
4. K. F. Janz, J. D. Dawson, L. T. Mahoney, Predicting heart growth during puberty: The Muscatine Study. *Pediatrics* **105**, E63 (2000).
5. C. G. Pham *et al.*, Striated muscle-specific beta(1D)-integrin and FAK are involved in cardiac myocyte hypertrophic response pathway. *Am J Physiol Heart Circ Physiol* **279**, H2916-2926 (2000).
6. H. A. Rockman, W. J. Koch, R. J. Lefkowitz, Seven-transmembrane-spanning receptors and heart function. *Nature* **415**, 206-212 (2002).
7. O. F. Bueno *et al.*, The MEK1-ERK1/2 signaling pathway promotes compensated cardiac hypertrophy in transgenic mice. *The EMBO journal* **19**, 6341-6350 (2000).
8. N. Frey, E. N. Olson, Cardiac hypertrophy: the good, the bad, and the ugly. *Annual review of physiology* **65**, 45-79 (2003).
9. P. Almeida *et al.*, B-type natriuretic peptide and left ventricular hypertrophy in hypertensive patients. *Revista portuguesa de cardiologia : orgao oficial da Sociedade Portuguesa de Cardiologia = Portuguese journal of cardiology : an official journal of the Portuguese Society of Cardiology* **22**, 327-336 (2003).
10. S. C. Kolwicz, R. Tian, Glucose metabolism and cardiac hypertrophy. *Cardiovascular Research* **90**, 194-201 (2011).
11. N. Milani-Nejad, P. M. L. Janssen, Small and large animal models in cardiac contraction research: advantages and disadvantages. *Pharmacology & therapeutics* **141**, 235-249 (2014).
12. J. A. Thomson *et al.*, Embryonic stem cell lines derived from human blastocysts. *Science (New York, N.Y.)* **282**, 1145-1147 (1998).
13. G. Holmgren *et al.*, Long-term chronic toxicity testing using human pluripotent stem cell-derived hepatocytes. *Drug metabolism and disposition: the biological fate of chemicals* **42**, 1401-1406 (2014).
14. A. Lundin *et al.*, Human iPS-Derived Astroglia from a Stable Neural Precursor State Show Improved Functionality Compared with Conventional Astrocytic Models. *Stem cell reports* **10**, 1030-1045 (2018).

15. I. M. E. Geraets *et al.*, Human embryonic stem cell-derived cardiomyocytes as an in vitro model to study cardiac insulin resistance. *Biochimica et biophysica acta. Molecular basis of disease* **1864**, 1960-1967 (2018).
16. X. Wu *et al.*, Local InsP3-dependent perinuclear Ca2+ signaling in cardiac myocyte excitation-transcription coupling. *J Clin Invest* **116**, 675-682 (2006).
17. S. Kim, H. Iwao, Molecular and cellular mechanisms of angiotensin II-mediated cardiovascular and renal diseases. *Pharmacological reviews* **52**, 11-34 (2000).
18. G. Foldes *et al.*, Modulation of human embryonic stem cell-derived cardiomyocyte growth: a testbed for studying human cardiac hypertrophy? *J Mol Cell Cardiol* **50**, 367-376 (2011).
19. A. Tanaka *et al.*, Endothelin-1 induces myofibrillar disarray and contractile vector variability in hypertrophic cardiomyopathy-induced pluripotent stem cell-derived cardiomyocytes. *J Am Heart Assoc* **3**, e001263 (2014).
20. P. Aggarwal *et al.*, RNA expression profiling of human iPSC-derived cardiomyocytes in a cardiac hypertrophy model. *PloS one* **9**, e108051 (2014).
21. A. P. Davenport *et al.*, Endothelin. *Pharmacological reviews* **68**, 357-418 (2016).
22. E. Ovchinnikova *et al.*, Modeling Human Cardiac Hypertrophy in Stem Cell-Derived Cardiomyocytes. *Stem cell reports*, (2018).
23. T. P. Dias *et al.*, Biophysical study of human induced Pluripotent Stem Cell-Derived cardiomyocyte structural maturation during long-term culture. *Biochemical and biophysical research communications*, (2018).
24. T. Kamakura *et al.*, Ultrastructural Maturation of Human-Induced Pluripotent Stem Cell-Derived Cardiomyocytes in a Long-Term Culture. *Circulation Journal* **77**, 1307-1314 (2013).
25. S. D. Lundy, W.-Z. Zhu, M. Regnier, M. A. Laflamme, Structural and Functional Maturation of Cardiomyocytes Derived from Human Pluripotent Stem Cells. *Stem Cells and Development* **22**, 1991-2002 (2013).
26. G. Foldes *et al.*, Aberrant alpha-adrenergic hypertrophic response in cardiomyocytes from human induced pluripotent cells. *Stem cell reports* **3**, 905-914 (2014).
27. J. Lewandowski *et al.*, The impact of in vitro cell culture duration on the maturation of human cardiomyocytes derived from induced pluripotent stem cells of myogenic origin. *Cell Transplant* **27**, 1047-1067 (2018).
28. O. Zolk, F. Munzel, T. Eschenhagen, Effects of chronic endothelin-1 stimulation on cardiac myocyte contractile function. *Am J Physiol Heart Circ Physiol* **286**, H1248-1257 (2004).
29. E. Ovchinnikova *et al.*, Modeling Human Cardiac Hypertrophy in Stem Cell-Derived Cardiomyocytes. *Stem cell reports* **10**, 794-807 (2018).
30. A. T. Mikhailov, M. Torrado, The enigmatic role of the ankyrin repeat domain 1 gene in heart development and disease. *The International journal of developmental biology* **52**, 811-821 (2008).
31. I. Herrer *et al.*, RNA-sequencing analysis reveals new alterations in cardiomyocyte cytoskeletal genes in patients with heart failure. *Laboratory Investigation* **94**, 645-653 (2014).
32. E. Lara-Pezzi *et al.*, Expression of follistatin-related genes is altered in heart failure. *Endocrinology* **149**, 5822-5827 (2008).
33. M. Shimano *et al.*, Cardiac Myocyte-specific Ablation of Follistatin-like 3 Attenuates Stress-induced Myocardial Hypertrophy. *Journal of Biological Chemistry* **286**, 9840-9848 (2011).
34. J. Ye *et al.*, Increased Interleukin-11 Levels Are Correlated with Cardiac Events in Patients with Chronic Heart Failure. *Mediators of inflammation* **2019**, 1575410 (2019).

35. S. Schafer *et al.*, IL-11 is a crucial determinant of cardiovascular fibrosis. *Nature* **552**, 110 (2017).
36. I. Fernández-Ruiz, IL-11 is a potential therapeutic target in cardiovascular fibrosis. *Nature Reviews Cardiology* **15**, 1 (2017).
37. G. Holmgren *et al.*, Identification of stable reference genes in differentiating human pluripotent stem cells. *Physiological Genomics* **47**, 232-239 (2015).
38. N. Ghosheh *et al.*, Highly Synchronized Expression of Lineage-Specific Genes duringIn VitroHepatic Differentiation of Human Pluripotent Stem Cell Lines. *Stem Cells International* **2016**, 1-22 (2016).
39. R Core Team (2019). R: A language and environment for statistical computing. R Foundation for Statistical Computing, Vienna, Austria. URL https://www.R-project.org/. (2019).
40. M. D. Robinson, D. J. McCarthy, G. K. Smyth, edgeR: a Bioconductor package for differential expression analysis of digital gene expression data. *Bioinformatics* **26**, 139-140 (2009).
41. H. Heberle, G. V. Meirelles, F. R. Da Silva, G. P. Telles, R. Minghim, InteractiVenn: a web-based tool for the analysis of sets through Venn diagrams. **16**, (2015).